Emission Efficiency Dependence on the Tilted Angle of Nanogaps in Surface Conduction Electron-Emitter

Yiming Li*, Yi-Ting Kuo, Hui-Wen Cheng, Ta-Ching Yeh, Hsiang-Yu Lo, Mei-Tsao Chiang[1], and Chi-Neng Mo[1]
Department of Communication Engineering, National Chiao Tung University, Hsinchu City, Taiwan
[1]TFT-LCD R&D Center, Chunghwa Picture Tubes, Ltd., Taoyuan, Taiwan
*E-mail: ymli@faculty.nctu.edu.tw

***Abstract*—In this work, the emission efficiency of the novel surface conduction electron-emitter corresponding to tilted angles (θ) of the driving electrode is studied numerically. Due to the small angle, the emitter apex becomes significant and induces large electric field. The large electric field then attracts more particles into vacuum and then increases the emission current. However, the structure of the driving electrode limits the electron trajectory while the angle decreases, and it reflects the portion of collected current by the anode decreases and makes a drop in emission efficiency. It shows there is the highest emission efficiency (about 37%) under an optimum angle θ = 60°. The result provides an insight into the relation between emission efficiency and emitter apex.**

Keywords-Nanogap, Surface Conduction Electron-Emitter, Emission Efficiency, Maxwell Equation, Fowler-Nordheim Equation, FDTD, Particle-in-Cell, Emitted Current, Collected Current by Anode.

I. INTRODUCTION

Surface conduction electron-emitter display (SED) features lower material costs than LCD, so the manufacturing costs could be reduced. Electrodes with nanometer separation have diverse applications, such as molecular electronics [1] and vacuum microelectronics [2]. One of emerging technologies of nanogap is the surface conduction electron emitter (SCE) for the flat panel displays (FPDs) applications which has attracted much attention since reported by Sakai [3]. The SCE display (SED) is an advanced type of FPD based upon SCEs. The critical process step to fabricate SCEs is to create a nanofigure on a line electrode for the electron emission. SEDs have high quality image, high resolution, quick response time, as well as low power consumption [4], but the nanogap fabrication process is complicated and expensive. The field emission (FE) efficiency and current density of these FE cathodes further depend on both their geometry and fabrication materials. For the SCE, emission is obtained with a large electric field by a driving voltage that causes electrons to tunnel over a potential barrier out of the emitter to the driving electrode and anode. The emitter's geometry increases emission by enhancing the electric field and reducing the barrier over which the electrons must tunnel. A novel SCE device has been proposed and studied for its high emission efficiency [5-8]. The emission efficiency strongly depends on the emitter's geometry and tilted angle.

In this work, the effect of angle of driving electrode on FE performance is examined by solving a set of Maxwell equations and Lorentz equation with the finite-difference time-domain particle-in-cell (FDTD-PIC) method [5-8]. In the FE process, the electron emission is modeled by the Fowler-Nordheim equation. As the tiled angle (θ) of the Fig. 1 decreases, the emitter apex will gather the high electric field, and which introduces high emission current. But the geometry will also limit the particle trajectory and reduce the collected current on the anode. The optimum angle is thus examined for the high emission efficiency of novel SCE device. This paper is organized as follows. We state the structure of SEDs and simulation technique in Sec. II. Simulation results and discussion on the emission properties are shown in Sec. III. Finally, we conclude the result that there is an optimum angle for the best emission efficiency.

II. STRUCTURE AND SIMULATION TECHNIQUE

The configurations for novel SCE devices are shown in Fig. 1 (a), which 87 nm is an experimentally empirical value. The driving voltage is 40 V and the voltage between the cathode and anode is 2000 V.

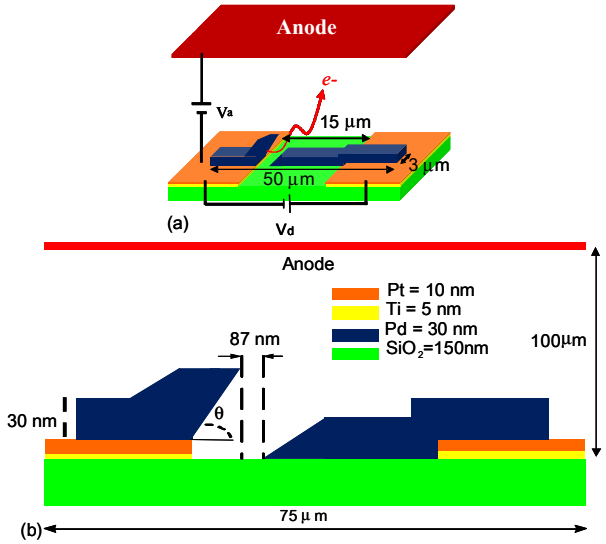

Figure 1. (a) The structure of novel SCE devices. (b) The whole device width is 75 um and the nanogap separation of D is varied. The driving voltage is 40 V and the voltage between the cathode and anode is 2000 V.

The simulated time is set as 0.017 ps, at that time the applied voltage is stable. The SCE device is solved using FDTD-PIC simulation technique [5-8]. We first formulate a calibration model with the experimental data by using the

978-1-4244-1753-7/08/$25.00 ©2008 IEEE

simulation program which has been developed to calculate the emission efficiency of different SCEs. The electromagnetic particle-in-cell codes are performed in the numerical simulation, where the computational flowchart is shown in Fig. 2. Starting from a specified initial state, we simulate electrostatic fields as its evolution in time. We then perform a time integration of Faraday's law, Ampere's law, and the relativistic Lorentz equation [9, 10],

$$\begin{cases} \dfrac{\partial \mathbf{B}}{\partial t} = -\nabla \times \mathbf{E}, \\ \dfrac{\partial \mathbf{E}}{\partial t} = -\dfrac{\mathbf{J}}{\varepsilon} + (\mu\varepsilon)^{-1}\nabla \times \mathbf{B}, \\ \mathbf{F} = q(\mathbf{E} + \mathbf{v} \times \mathbf{B}), \text{ and} \\ \dfrac{\partial \mathbf{x}}{\partial t} = \mathbf{v}, \end{cases} \tag{1}$$

subject to constraints provided by Gauss's law and the rule of divergence of B,

$$\nabla \cdot \mathbf{E} = \frac{\rho}{\varepsilon} \text{ and } \nabla \cdot \mathbf{B} = 0. \tag{2}$$

We notice that **E** and **B** are the electric and magnetic fields, **x** is the position of charge particle, and J and ρ are the current density and charge density resulting from charge particles. The full set of time-dependent Maxwell equations is simultaneously solved to obtain electromagnetic fields. Similarly, the Lorentz force equation is solved to obtain relativistic particle trajectories. In addition, the electromagnetic fields are advanced in time at each time step. The charged particles are moved according to the Lorentz equation using the fields advanced in each time step. The weighted charge density and current density at the grids are subsequently calculated. The obtained charge density and current density are successively used as sources in the Maxwell equations for advancing the electromagnetic fields. These steps are repeated for each time step until the specified number of time steps is reached. We notice that the space-charge effects are automatically included in the simulation algorithms. The effect of space charge on field emission was discussed by Stern, Gosling, and Fowler [9]. This FDTD-PIC method [11-13] thus approaches to self-consistent simulation of the electromagnetic fields and charged particles.

In the field emission process, the electron emission is modeled by the Fowler-Nordheim (F-N) equation [8],

$$J = \frac{AE^2}{\varphi t^2} \exp\left(\frac{-Bv(y)\varphi^{\frac{3}{2}}}{E}\right), \tag{3}$$

where $A = 1.541 \times 10^{-6}$ A eV/V^2 and $B = 6.3408 \times 10^8$ eV$^{-3/2}$ V um^{-1}, E is the normal component of the electric field at the emitter surface, φ is the work function of the emission material, t^2 is approximately equal to 1.1, and $v(y) = 0.95 - y^2$ with $y = 3.79 \times 10^{-5} \times E^{1/2} / \varphi$ is in SI unit. The emission current density is determined by Eq. (3) according to the local electric field, the work function of emitter material, and the geometric factors. We notice that, in the entire simulation, all dimensions of physical quantities are the same with the experimental settings [5-8].

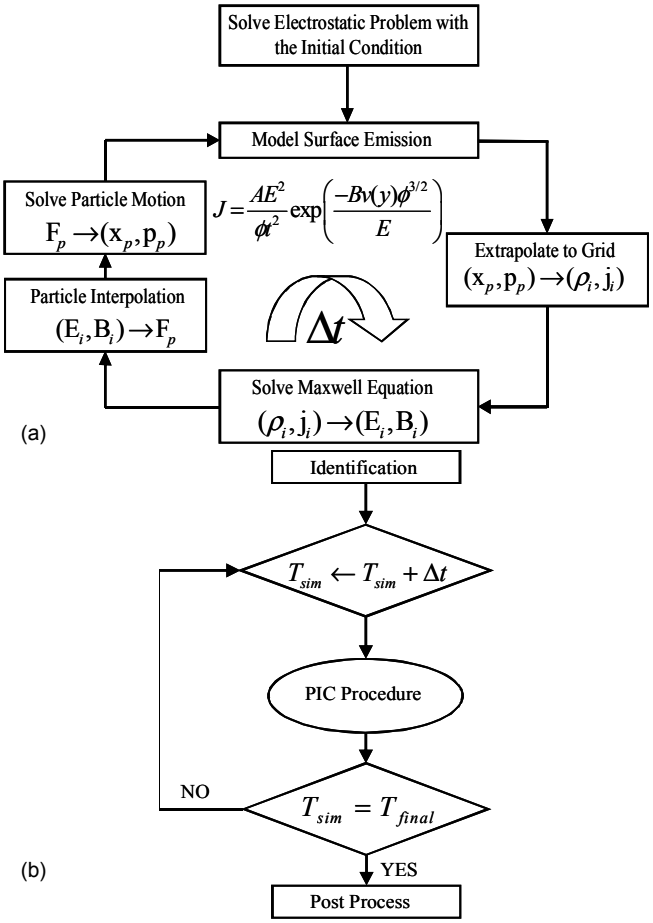

Figure 2. (a) The flowchart for the PIC procedure. (b) The computational scheme for the simulation, where the block of the PIC procedure is shown.

III. Results and Discussion

As the angle decreases, the emitter apex gradually becomes significant and the around electric field increases. The electric fields of the explored structure under a tilted angle of 60^o are shown in Fig. 3. The large electric field can be observed at the emitter apex with θ = 15^o, where the tip of electric field is 2.10×10^9, as shown in Fig. 4. It expresses the extension of emitter apex and gathers a large electric field than the device with θ = 60^o, where the tip of electric field is 1.81×10^9. In the beginning, the electrons will be emitted from Palladium (Pd) [14]; when the anode voltage is increased, the emitted electrons will be attracted upward. When the anode voltage continuously keeps increasing, electrons will keep moving upward. Finally, the most of emitted electrons will be collected by the top anode, as shown in Fig. 5, for the case of θ = 60^o.

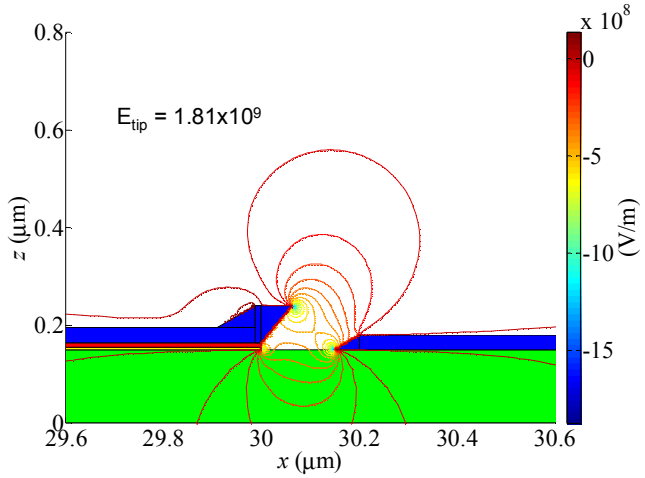

Figure 3. Contours of the electric fields of the structure with the θ = 60° and 87 nm nanogap at Vd = 40 V.

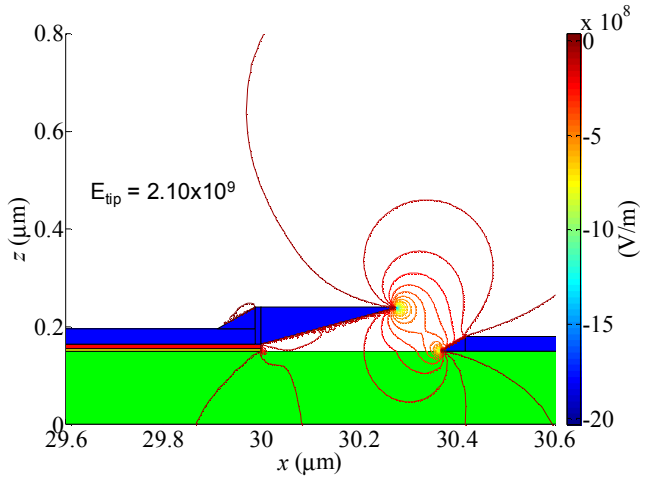

Figure 4. Contours of the electric fields of the structure with the θ = 15° and 87 nm nanogap at Vd = 40 V.

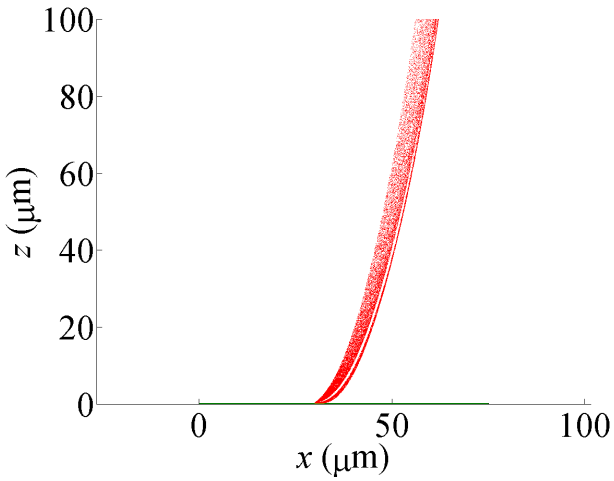

Figure 5. Electron trajectory of the structure with the θ = 60° and 87 nm nanogap at Vd = 40 V.

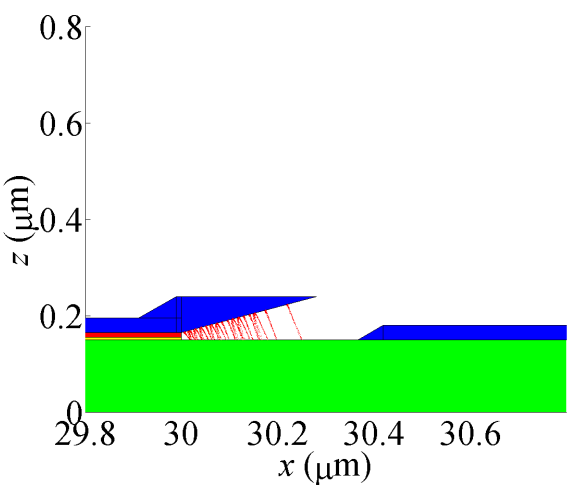

Figure 6.. The electron emission of the structure with the θ = 15° and 87 nm nanogap at Vd = 40 V.

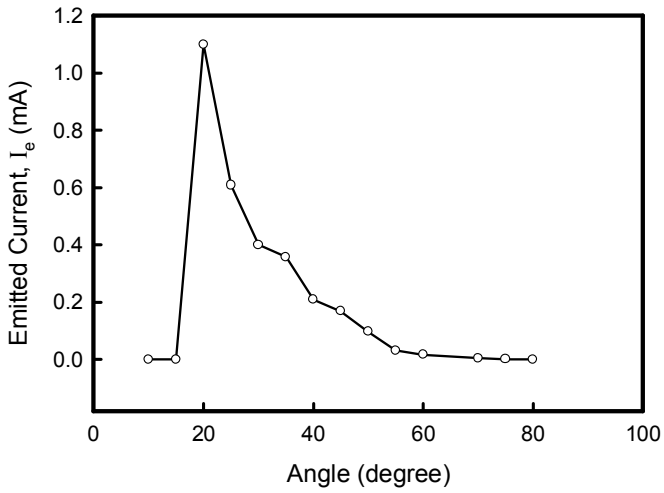

Figure 7. The emission current versus the tilted angles.

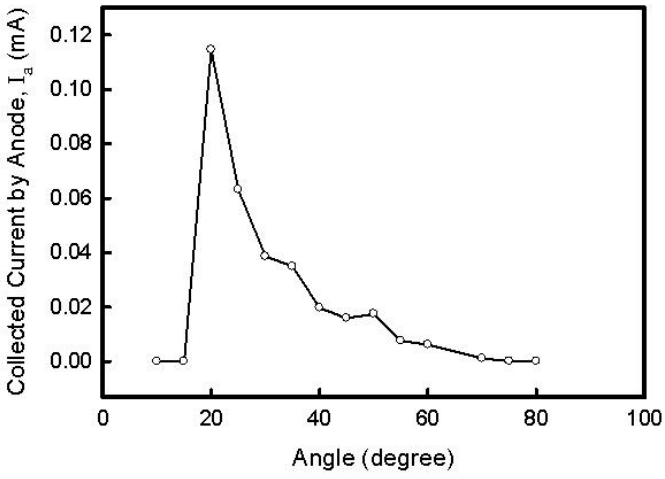

Figure 8. The corresponding collected current by the top anode plate versus the tilted angles.

However, the geometry of emitter apex under small angle limits the electron trajectory, as shown in Fig. 6. It expresses the extension of emitter apex gather a large electric field than the device under the angle of 60°. However, the geometry of emitter apex under small angle limits the electron trajectory, as shown in Fig. 6. The electron trajectories of the cross section on the *xz* plane vary as the angles change, and the emission efficiency is then affected. The reason of the efficiency changes can be expressed by the emission current of the driving electrode and the collected current by anode.

Figure 7 shows the emission current under different angles. While the angle decreases, the expected large electric field will gather around the emitter apex, and then more particles are attracts into vacuum and transmit to the opposite electrode. Hence the emission current increases. However, the increasing emission current does not imply the increasing emission efficiency due to the structure of the device. It is because the extension of the driving electrode limits the electron trajectories while the angle decreasing, such that even the more particles are attracted into vacuum, the portion of the particles collected by the anode does not increasing linearly. The collected current by the anode is shown in Fig. 8, and the emission efficiency is shown in Fig. 9. To evaluate the emission efficiency, we use the ratio of emission current and collected current by the anode plate:

$$\text{Emission Efficiency} = \frac{\text{Collected Current by Anode}}{\text{Emission Current}}. \quad (4)$$

The emission efficiency behaves nonlinear corresponding to varying angles of the driving electrode, and there exists an optimum angle, as shown in Fig. 9. There is a best emission efficiency about 37 % for the structure with $\theta = 60^{o}$.

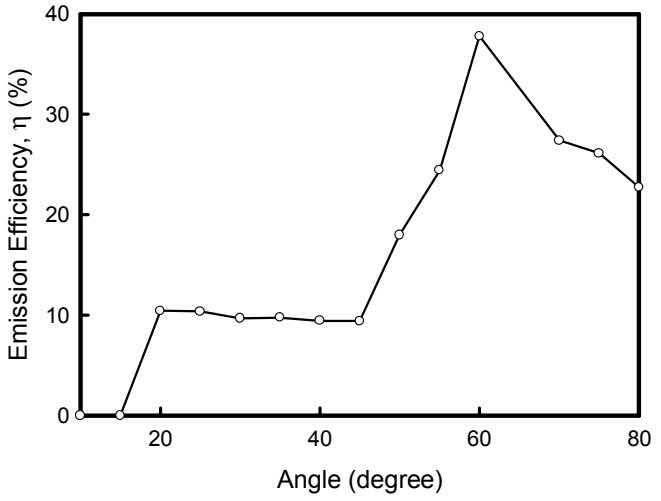

Figure 9. Dependence of the field emission efficiency on different titled angles.

IV. Conclusions

The emission efficiency for the novel SCE corresponding to the titled angles of the driving electrode has been studied. To estimated the electron trajectory, the emission and collected currents and the emission efficiency, a set of Maxwell equation and Fowler-Nordheim equation has been solved numerically with the finite-difference time-domain particle-in-cell method Due to the small angle, the emitter apex is significant which induces large electric field. The large electric field then has attracted more particles into vacuum and then increases the emission current. However, the structure of the driving electrode limited the electron trajectory while the tilted angle has decreased, and it has reflected the portion of collected current by the top anode decreases, and thus suppresses the emission efficiency. An optimum tilted angle of the novel SCE device $\theta = 60^{o}$ has been determined for the fixed separation width of the nanogap. For global optimal configuration of the three-dimensional structure, we are currently including more variables in the simulation model.

Acknowledgment

This work was supported in part by Taiwan National Science Council (NSC) under Contract NSC-96-2221-E-009-210 and Contract NSC-96-2752-E-009-003-PAE, and by the Chunghwa Picture Tubes under a 2006-2008 grant.

References

[1] M. A. Reed, C. Zhou, C. J. Muller, T. P. Burgin, and J. M. Tour, "Conductance of a molecular junction," *Science*, vol. 278, no. 5336, pp. 252-254, Oct. 1997.

[2] H. I. Lee, S. S. Park, D. I. Park, S. H. Ham, J. H. Lee, and J. H. Lee, "Nanometer-scaled gap control for low voltage and high current operation of field emission array," *J. Vac. Sci. Technol. B*, vol. 16, no. 2, pp. 762-764, Mar. 1998.

[3] K. Sakai, I. Nomura, E. Yamaguchi, M. Yamanobe, S. Ikeda, T. Hara, K. Hatanaka, Y. Osada, H. Yamamoto, and T. Nakagiri, "Flat-panel displays based on surface-conduction electron-emitters," in *Proc. of EuroDisplay*, 1996, pp. 569-572.

[4] E. Yamaguchi, K. Sakai, I. Nomura, T. Ono, M. Yamanobe, N. Abe, T. Hara, K. Hatanaka, Y. Osada, H. Yamamoto, and T. Nakagiri, "A 10-in. surface-conduction electron-emitter display," *J. Soc. Inf. Disp.*, vol. 5, no. 4, pp. 345-348, 1997.

[5] H.-Y. Lo, Y. Li, H.-Y. Chao, C.-H. Tsai, F.-M. Pan, "Field Emission Properties of Novel Palladium Nanogaps for Surface Conduction Electron-Emitters," *Nanotechnology* 18, 475708, 2007.

[6] Y. Li and H.-Y. Lo, "Surface Conduction Electron Emission in Palladium Hydrogenation Nanogaps," *J. Phys. D. Appl. Phys*. 41, 085301, 2008.

[7] Y. Li, H.-Y. Chao, and H.-Y. Lo, *J. Compu. Electronics*, at press, 2008. doi: 10.1007/s10825-007-0168-0.

[8] H-Y Lo, Y. Li, C-H Tsai, H-Y Chao, and F-M Pan, "Effect of Process Variation on Field Emission Characteristics in Surface Conduction Electron-Emitters," to appear in *IEEE Trans. on Nanotech.*

[9] Y. Goth, T. Ohtake, N. Fujita, K. Inoue, H. Tsuji, and J. Ishikawa, "Fabrication of Lateral-type Thin-film Edge Field Emitters by Focus Ion Beam Technique," *J. Vac. Sci. Technol. B*, vol. 13, no. 2, pp. 465-468, 1995.

[10] T. E. Stern, B. S. Gosling, and R. H. Fowler, "Further studies in the emission of electrons from cold metals," *Roy. Soc. Proc. A*, vol. 124, no. 795, pp. 699-723, July 1929.

[11] J. P. Verboncoeur, A. B. Langdon and N. T. Gladd, "An object-oriented electromagnetic PIC code," *Comput. Phys. Commun.* vol. 87, pp. 199-211, 1995.

[12] B. Goplen, L. Ludeking, D. Smithe and G. Warren, "User-configurable MAGIC for electromagnetic PIC calculations," *Comput. Phys. Commun.* vol. 87, pp. 54-86, 1995.

[13] C. K. Birdsall and A. B. Langdon, *Plasma Physics via Computer Simulation* (New York: McGraw-Hill), 1985.

[14] H. B. Michaelson, "The work function of the elements and its periodicity," *J. Appl. Phys.* vol. 48, pp. 4729-33, 1977.